

# Self-consistent description of cold fission processes

D. S. Delion<sup>1</sup>, A. Săndulescu<sup>2</sup>, Ș. Mișicu<sup>1,3</sup>, and W. Greiner<sup>3</sup>

<sup>1</sup>National Institute of Physics and Nuclear Engineering  
Bucharest-Măgurele, POB MG-6, Romania

<sup>2</sup>Center for Advanced Studies in Physics  
Romanian Academy, Calea Victoriei, 125, Bucharest, Romania

<sup>3</sup>Institut für Theoretische Physik, J.W.v.-Goethe  
Universität, Robert Mayer str. 8-10, Frankfurt, Germany

November 20, 2002

## Abstract

We give a description of cold fission processes within the stationary scattering formalism. We predict a strong dependence of binary decay widths for  $^{252}\text{Cf}$  upon the internal structure of the considered resonant state. We also describe the spontaneous ternary cold fission of  $^{252}\text{Cf}$ , accompanied by  $^4\text{He}$ ,  $^{10}\text{Be}$  and  $^{14}\text{C}$ . We have shown that angular distribution of the emitted light particle is strongly connected with its deformation and the equatorial distance.

## 1 Introduction

The use of the Gammasphere and Eurogam facilities in the last years offered the possibility to explore the cold (neutronless) binary and ternary fission of  $^{252}\text{Cf}$  [1, 2, 3, 4]. The triple  $\gamma$ -rays coincidence technique enabled the identification of this rare cold fission process. They confirm the theoretical predictions based on the idea of the cold rearrangements of large clusters of nucleons from the initial to the final ground states, similar to the cluster radioactivity phenomenon [5, 6].

In the binary fission the knowledge of the spin distribution of the emitted fragments is very important because it provides an important information concerning the fissioning system in the region of the scission point. A model for explaining the population of fragment rotational states has been laid down by Rasmussen et al. [7]. It is considered, as the only reasonable ground for discarding the fragment orientation fluctuations, such as bending and wriggling [8], a neck which eventually breaks off the fission axis.

The first aim of this paper is to describe the binary cold fission process of  $^{252}\text{Cf}$  as a decay of a resonant state. We calculate the yields of the rotational states in coincidence within a stationary scattering theory.

Recently a new experiment was performed by a joint collaboration (Vanderbilt, Berkeley and Dubna) [9] allowing the measurement of the averaged energy and the angular distribution of light clusters in the ternary fission of  $^{252}\text{Cf}$ . Several theoretical approaches

were devoted to this subject [10, 11, 12]. In Refs. [13, 14] we proposed a microscopic treatment of the ternary fission process.

Our second goal is to explain for ternary fission why the averaged values of energy spectra for different light clusters are so close to each other. The angular distributions are centered practically around the same angle for all emitted light clusters. Therefore another goal is to describe this very precise anisotropy.

## 2 Theoretical background

### 2.1 Binary fission

The dynamics of the cold fission is described as a two-body decay process. Let us denote by  $\mathbf{R} = (R, \hat{R})$  the distance between the centers of two deformed nuclei. The orientation of their major axes is given by the Euler angles  $\Omega_k = (\varphi_k, \theta_k, 0)$ ,  $k = 1, 2$ . We describe the dynamics of the decay process by a stationary Schrödinger equation

$$H\Psi(\mathbf{R}, \Omega_1, \Omega_2) = E\Psi(\mathbf{R}, \Omega_1, \Omega_2) . \quad (2.1)$$

The Hamiltonian operator can be written in two different ways, depending on the distance  $\mathbf{R}$ . In the external region, beyond some radius  $R > R_c$ , we consider that each nucleus is left in some excited rotational state

$$H = -\frac{\hbar^2}{2\mu}\nabla_{\mathbf{R}}^2 + H_1(\Omega_1) + H_2(\Omega_2) + V(\mathbf{R}, \Omega_1, \Omega_2) , \quad (2.2)$$

where  $\mu$  is the reduced mass and  $H_k(\Omega_k)$  are the Hamiltonians describing the rotation of the fragments. We estimate the interaction between nuclei using the double folding between nuclear densities [15], where as a nucleon-nucleon force we use M3Y interaction [16]. For smaller distances  $R < R_c$  the two nuclear densities overlap each other. The two nuclei oscillate around the pole-to-pole position because the potential increases as a function of angles. This is the most favourable fissioning configuration with the smallest Coulomb barrier. By considering only the angles  $\theta_1, \theta_2$  and taking  $\varphi_1 = \varphi_2 = 0$  we expand the potential around this relative configuration. In this way one obtains

$$H = -\frac{\hbar^2}{2\mu}\frac{1}{R}\frac{\partial^2}{\partial R^2}R + H_1(R, \theta_1) + H_2(R, \theta_2) + H_{12}(R, \theta_1, \theta_2) + V_{p-p}(R) , \quad (2.3)$$

where  $H_k(R, \theta_k)$  describe harmonic oscillations,  $H_{12}(R, \theta_1, \theta_2)$  is the coupling term, as given in Ref. [17] and  $V_{p-p}$  is the pole-pole potential.

The wave functions satisfying the Schrödinger equation in the two regions are given respectively by

$$\begin{aligned} \Psi(\mathbf{R}, \Omega_1, \Omega_2) &= \frac{1}{R} \sum_{I_1 I_2} \mathcal{R}_{I_1 I_2}(R) \mathcal{Y}_{I_1 I_2}(\hat{R}, \Omega_1, \Omega_2), \quad R > R_c , \\ \Psi(R, \theta_1, \theta_2) &= \frac{1}{R} \sum_{n_1 n_2} \mathcal{R}_{n_1 n_2}(R) \mathcal{Z}_{n_1 n_2}(\theta_1, \theta_2), \quad R < R_c . \end{aligned} \quad (2.4)$$

The angular parts of these functions are defined by

$$\begin{aligned} \mathcal{Y}_{I_1 I_2}(\hat{R}, \Omega_1, \Omega_2) &= \left\{ Y_l(\hat{R}) \otimes [\Phi_{I_1}(\Omega_1) \otimes \Phi_{I_2}(\Omega_2)]_l \right\}_0 , \\ \mathcal{Z}_{n_1 n_2}(\theta_1, \theta_2) &= \Phi_{n_1}(\theta_1) \Phi_{n_2}(\theta_2) . \end{aligned} \quad (2.5)$$

Here  $\Phi_{I_k}$  are the normalized Wigner functions [18] and  $\Phi_{n_k}$  the harmonic oscillator wave functions. They satisfy the following eigenvalue equations

$$\begin{aligned} H_k \Phi_{I_k M_k}(\Omega_k) &= E_{I_k} \Phi_{I_k M_k}(\Omega_k), \quad R > R_c, \\ H_k \Phi_{n_k}(\theta_k) &= E_{n_k} \Phi_{n_k}(\theta_k), \quad R < R_c. \end{aligned} \quad (2.6)$$

By using the orthonormality of the angular functions entering the superpositions (2.4) one obtains in a standard way a coupled system of differential equations for the radial components

$$\frac{d^2 \mathcal{R}_l}{d\rho_l^2} = \sum_{l'=1}^N \mathcal{A}_{l;l'} \mathcal{R}_{l'}, \quad l = 1, \dots, N, \quad (2.7)$$

where we used a short-hand notation for the channel index

$$l = (l, I_1, I_2), \quad R > R_c, \quad = (n_1, n_2), \quad R < R_c. \quad (2.8)$$

The coupling matrix is given in Ref. [19]. We find the resonant states using the standard technique.

The decay width for some channel  $l$  is twice the imaginary part of the resonant energy, but can also be derived from the continuity equation in a straightforward way

$$\Gamma_l = \hbar v_l \lim_{R \rightarrow \infty} |\mathcal{R}_l(R)|^2 = \hbar v_l |S_l|^2, \quad (2.9)$$

where  $S_l$  are the coefficients multiplying the outgoing Coulomb waves and  $v_l$  is the center of mass velocity at infinity in the channel  $l$ .

## 2.2 Ternary fission

The Hamiltonian of the ternary fission process can be written as follows

$$H = -\frac{\hbar^2}{2\mu_{12}} \nabla_R^2 - \frac{\hbar^2}{2\mu_3} \nabla_r^2 + V^{(12)}(R) + V^{(3)}(R, \mathbf{r}). \quad (2.10)$$

The total wave function

$$\psi_K(\mathbf{R}, \mathbf{r}) = \sum_n \psi_{nK}^{(12)}(\mathbf{R}) \psi_{n-K}^{(3)}(R, \mathbf{r}), \quad (2.11)$$

where  $n$  denotes the eigenvalue resonance number and  $K$  the angular momentum projection on the intrinsic axis, satisfies the stationary Schrödinger equation

$$H \psi_K(\mathbf{R}, \mathbf{r}) = E_K \psi_K(\mathbf{R}, \mathbf{r}). \quad (2.12)$$

For some distance between heavy fragment  $R$  the motion of the light particle is given by

$$\left[ -\frac{\hbar^2}{2\mu_3} \nabla_r^2 + V^{(3)}(R, \mathbf{r}) - E_{nK}^{(3)}(R) \right] \psi_{nK}^{(3)}(R, \mathbf{r}) = 0. \quad (2.13)$$

Therefore the motion of the two heavy fragments is governed by

$$\left[ -\frac{\hbar^2}{2\mu_{12}} \nabla_R^2 + V^{(12)}(R) + E_{nK}^{(3)}(R) - E_K \right] \psi_{nK}^{(12)}(\mathbf{R}) = \sum_{n'} \mathcal{A}_{n-K, n'-K}(R) \psi_{n'K}^{(12)}(\mathbf{R}), \quad (2.14)$$

where  $\mathcal{A}_{nK,n'K'}(R)$  is called the adiabatic matrix [20].

The potential  $V^{(12)}$  acting between heavy clusters is given by a double folding procedure using Coulomb+M3Y nuclear interaction. The position of the first resonant state is adjusted by a repulsive core [19]. The potential acting on the light cluster is a sum of the Coulomb and nuclear parts. The nuclear potential is given by a deformed harmonic oscillator (ho) shape

$$V_N^{(3)}(x, z) = -V_0 + v \frac{\hbar^2}{2\mu_3} \beta^2 \left[ \left(1 + \frac{4}{3}\delta\right)(x - x_0)^2 + \left(1 - \frac{2}{3}\delta\right)(z - z_0)^2 \right]. \quad (2.15)$$

The ho parameter of the light cluster is defined in a standard way [21]. We estimate  $z_0$  as the half distance between nuclear surfaces at  $x_0=0$  [20]. The factor  $v$  is a scaling parameter.

The probability that the light particle is emitted in some direction  $\theta$  is given by the continuity equation

$$\Gamma_{nK}^{(3)}(R, \theta) = \hbar v_{nK} \lim_{r \rightarrow \infty} |r \psi_{nK}^{(3)}(R, \mathbf{r})|^2 = \Gamma_{nK}^{(3)}(R) W_{nK}^{(3)}(R, \theta), \quad (2.16)$$

where  $v_{nK}$  is the light particle velocity at infinity and  $\Gamma_{nK}^{(3)}(R)$  the integrated width. Angular distribution is given by

$$W_{nK}^{(3)}(R, \theta) = \sum_L A_{nLK} Y_{L0}(\theta), \quad (2.17)$$

in terms of  $A_{nLK}$  coefficients derived in Ref. [20].

## 3 Numerical application

### 3.1 Binary fission

We studied the following splitting occurring in a binary cold fragmentation



with the decay energy  $Q=214.41$  MeV. The ground state deformations of the fragments are  $\beta_2 = 0.35$ ,  $\beta_4 = 0.03$  for  $^{104}\text{Mo}$  and  $\beta_2 = 0.24$ ,  $\beta_4 = 0.13$  for  $^{148}\text{Ba}$  [19, 22]. In the double folding expansion we considered M3Y + Coulomb interaction in a region where the sum of the densities is less than the equilibrium nuclear density. For shorter distances we simulated the Pauli repulsion by considering the double folding procedure with a contact delta force. We used the repulsive compression strength  $V_{\text{comp}}$  as a parameter in our analysis.

We considered that the internal (vibrational) region is separated from the external (rotational) region at the point where the spherical component of total interaction becomes smaller than the pole-to-pole interaction, i.e.  $R_c = 15.6$  fm. Here it becomes more favourable a rotation than a fixed aligned configuration.

First of all we considered that in the internal region the two fragments do not oscillate. In this case the role of the Coulomb excitations is negligible. In order to obtain nonvanishing contributions to the rotational states it is necessary to include angular oscillations of the two fragments in the internal region  $R < R_c$ .

We ordered the basis states by increasing the energy of the pairs  $E_{n_1} + E_{n_2}$ . These energies have a maximum corresponding to the minimum of the pocket potential. Around  $R_c$  they sharply decrease and intersect the energies of the rotational pairs.

It is possible in this way to connect one by one the two basis states.

We changed the value of the repulsive strength  $V_{\text{comp}}$ . In this way we were able to find several resonant states with an energy equal to the experimental  $Q$ -value. We then computed the decay widths to the final rotational states according to Eq. (2.9). In Figure 1 are given the total widths per nucleus versus the fragment angular momentum for the above considered resonances.

They are normalized to the first transition connecting the ground states. By solid lines we connected the values for  $^{104}\text{Mo}$  and by dashed lines for  $^{148}\text{Ba}$ . The experimental yields for  $^{104}\text{Mo}$  are 0.21[2<sup>+</sup>], 0.74(14)[4<sup>+</sup>], 0.05(5)[6<sup>+</sup>] and for  $^{148}\text{Ba}$  0.8[2<sup>+</sup>], 0.2(2)[4<sup>+</sup>] [2]. They are normalized to the total 2<sup>+</sup> + 4<sup>+</sup> + 6<sup>+</sup> yield. We denoted in round brackets the error and in squared brackets the angular momentum.

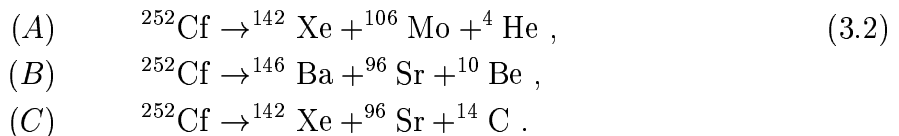
From Figure 1 we conclude that the third resonant state (0,3) is the closest to the experimental situation. We obtained a good agreement for the normalised yields of  $^{104}\text{Mo}$ : 0.22[2<sup>+</sup>], 0.67[4<sup>+</sup>], 0.11[6<sup>+</sup>]. Concerning  $^{148}\text{Ba}$  we obtained the values: 0.26[2<sup>+</sup>], 0.46[4<sup>+</sup>]. We mention that for this nucleus the experimental errors are larger.

The last state (1,2) has a similar distribution of the decay widths: 0.30[2<sup>+</sup>], 0.60[4<sup>+</sup>], 0.10[6<sup>+</sup>] for  $^{104}\text{Mo}$  and 0.11[2<sup>+</sup>], 0.61[4<sup>+</sup>] for  $^{148}\text{Ba}$ .

In order to discriminate between the two distributions it is necessary to have more information. To this aim we also predicted the widths considering the pairs of fragment angular momenta. Therefore these data are extremely important in understanding the dynamics of the cold fission process.

## 3.2 Ternary fission

We analyzed the following three ternary splittings of  $^{252}\text{Cf}$



We considered only the true cold (neutronless) fission process, i.e. the fragments are emitted in their ground states [20]. The energy spectra of emitted light fragments are centered around the values given in Table 1 (second column) [9].

**Table 1**

*The averaged values of energy spectra for the light fragment in the processes (3.2) are given in the second column. The widths are given in the third column and the angular distributions are centered around angles given in the fourth column. In the last two columns are given the  $Q$ -value and total kinetic energy of fragments (TKE), respectively.*

Process	$E$ (MeV)	$\Delta E$ (MeV)	$\theta_0$ (deg.)	$Q$ (MeV)	$TKE$ (MeV)
(A)	16	6	$84 \pm 1$	215.350	173
(B)	18	7	$84 \pm 2$	202.063	167
(C)	24	8	$83 \pm 2$	221.132	166

From this Table one can see that the averaged energies of emitted clusters are close to each other. It is also known that  $^{10}\text{Be}$  yields are by two orders of magnitudes less than for  $^4\text{He}$  [9]. This situation is in evident contrast with the cluster decay phenomenon because Coulomb barriers in the polar direction are very different.

A simple explanation can be given by the nuclear potential with parameters given in Table 2, having its minimum at  $x_0=6$  fm. This value is predicted by a microscopic estimate of Ref. [14] for  $R=12$  fm. This is the potential in which the light cluster is born.

**Table 2**

*The harmonic oscillator parameter  $b = 1/\beta^2$  for different emitted light fragments [21] (the second column),  $\beta = \mu_3\omega_0/\hbar$  (the third column) and the harmonic oscillator strength (the last column).*

Nucleus	$b$ (fm)	$\beta$ (fm $^{-2}$ )	$\frac{\hbar^2}{2\mu_3}\beta^2$ (MeV fm $^{-2}$ )
$^4\text{He}$	1.19	0.706	2.603
$^{10}\text{Be}$	1.44	0.480	0.481
$^{14}\text{C}$	1.65	0.367	0.201

The Coulomb barrier is strongly lowered in the case (B) and becomes comparable with the case (A). Indeed, in Table 2 one can see that the ho strength is by five times smaller in the second case. We estimated the first eigenvalue of this state versus the inter-fragment distance  $R$ . The depth of the h.o. potential,  $V_0=27.7$  MeV, reproduces the experimental value  $E^{(3)}=16$  MeV for  $R=15$  fm.

The predicted half-lives, corresponding to these dependencies for the eccentricity  $x_0=6$  fm, are of 2-3 order of magnitude above the characteristic nuclear time  $T_N = 10^{-22}$  s. This is consistent with the experimentally known fact that cold binary and  $\alpha$ -ternary yields are comparable and the corresponding half-lives are  $10^{-18}$  s [23].

Our numerical calculations showed that the adiabatic matrix is by one order of magnitude less than the energy of the light cluster resonant states. In our calculations we neglected it. Therefore the only coupling effect is the enhancement of the two-body Coulomb barrier between heavy fragments  $V^{(12)}(R) + E_{nK}^{(3)}(R)$ . The minimum of the inter-fragment potential is shifted to the left and the barrier is very much enlarged. The wave functions are concentrated around some given distance  $R$  between 12 and 14 fm and correspond to very large half-lives. Therefore the half-life of the whole ternary system is given by the shortest light particle half-life.

We studied the influence of different parameters of the nuclear potential (2.15) on the light cluster angular distribution. It turns out that it practically does not depend upon the inter-fragment distance  $R$ , the eccentricity  $x_0$ , the angular momentum projection  $K$  and the scaling parameter  $v$ .

In Fig. 2 we see that a small deviation from the equatorial parameter  $z_0$ , strongly changes the position of the maximum in the angular distribution. We stress on the fact that the choosen  $z_0$  gives a result very close to the experimental value in Table 1.

It is known that  $^{10}\text{Be}$  has a structure in terms of two  $\alpha$ -particles plus a neutron pair, and therefore should be very deformed. It is interesting to stress that by increasing deformation  $\delta$  the maximum approaches experimental value. In this way we conclude

that angular distribution is a tool to probe nuclear deformation, as it was already shown in  $\alpha$ -decay processes from odd-mass nuclei in Ref. [24].

The deformation of the light cluster potential has also an important effect on the half-life, because by increasing  $\delta$  the potential becomes flatter in the equatorial direction.

In the case of the process (C) an increasing of the parameter  $\delta$  changes the maximum, but the experimental value corresponds to  $\delta=0$ , which confirms the fact that  $^{14}\text{C}$  is not deformed.

## 4 Conclusions

In conclusion we developed a formalism to compute the decay probabilities to the final rotational states from the fissioning nucleus  $^{252}\text{Cf}$ . To this purpose we used the stationary scattering theory in finding the resonant states.

The mutual interaction of the two fragments was computed by using the double folding procedure with M3Y two-body plus Coulomb forces. For short distances between the fragments we simulated the Pauli principle by a repulsive delta-force core. By changing the repulsive strength it was possible to obtain different resonant states inside the resulting molecular potential.

The most favourable fissioning configuration is the pole-to-pole one. In the overlapping region the two fragments can oscillate around this equilibrium position.

We estimated the decay widths to the final rotational states using the standard stationary scattering formalism. It turns out that in the absence of any internal excitation the feeding of the excited states is vanishing. Only by inclusion of the internal angular oscillations around the pole-to-pole equilibrium position it becomes possible to generate rotational states. The values of the computed widths per nucleus as a function of the final spin are strongly dependent upon the considered resonant state.

Among the computed resonant states we found two possible candidates reproducing the available experimental yields. In order to discriminate between them we give a more detailed picture of the widths versus all possible pairs of the final angular momenta. We consider that the possibility to have these experimental yields would clarify the details concerning the molecular stage of  $^{252}\text{Cf}$ .

We analyzed new experimental data concerning the ternary emission of  $^4\text{He}$ ,  $^{10}\text{Be}$  and  $^{14}\text{C}$  from  $^{252}\text{Cf}$ . We answered the two main questions raised by experiment, namely

- 1) Why the energies and half-lives of the emitted light clusters are close to each other?
- 2) Why the angular distribution of the light clusters are centered around the same angle?

To answer the first question we supposed that the light cluster is born in the ho well with a size parameter given by its known nuclear density. Coulomb barriers in the equatorial direction become similar in the three cases, giving comparable eigenvalues of the first resonant states.

To answer the second question we analyzed the influence of all potential parameters on the maximum of the light particle angular distribution. It turns out that the only sensitive parameters are the deviation from the equator and the cluster deformation. From the position of the maximum in the angular distribution we concluded that the light cluster is born in the neck region. For  $^{10}\text{Be}$  we found out that a significant deformation improves the agreement with the experiment.

## References

- [1] G.M. Ter-Akopian, et al., Phys. Rev. Lett. **73**, 1477 (1994).
- [2] A. Săndulescu, A. Florescu, F. Cârstoiu, W. Greiner, J.H. Hamilton, A.V. Ramayya, and B.R.S. Babu, Phys. Rev. C **54**, 258 (1996).
- [3] A.V. Ramayya, et al., in Proceedings of the third International Conference "Dynamical Aspects of Nuclear Fission", Eds. J. Kliman and B.I. Pustylnik Častá-Papiernička, Slovak Republic, August 30-Sept 4, 1996, (JINR, Dubna, 1996) p307.
- [4] J.H. Hamilton, et al., in Proceedings of the Symposium on "Fundamental Issues in Elementary Matter" Ed. W. Greiner, Bad Honnef, Germany, September 25-29, 2000 (Ep Systema, Debrecen Hungary, 2000).
- [5] A. Săndulescu and W. Greiner, J. Physics G **3**, L189 (1977).
- [6] A. Săndulescu and W. Greiner, Rep. Prog. Phys. **55**, 1423 (1992).
- [7] J.O. Rasmussen, et al., in Proceedings of the third International Conference "Dynamical Aspects of Nuclear Fission", Eds. J. Kliman and B.I. Pustylnik Častá-Papiernička, Slovak Republic, August 30-Sept 4, 1996, (JINR, Dubna, 1996) p289.
- [8] J.R.Nix and W.J.Swiatecki, Nucl.Phys. **71**, 1 (1965).
- [9] G.M. Ter-Akopian, seminar 6 May, 2002, Frankfurt/Main.
- [10] A. Săndulescu, Ş Mişicu, F. Carstoiu, and W. Greiner, Fiz. Elem. Chastits Az. Yadra **30**, 908 (1999); Phys. Part. Nucl. **30**, 386 (1999).
- [11] A. Săndulescu, F. Carstoiu, I. Bulboacă, and W. Greiner, Phys. Rev. **C60**, 044613 (1999).
- [12] F. Carstoiu, I. Bulboacă, A. Săndulescu, and W. Greiner, Phys. Rev. **C61**, 044606 (2000).
- [13] A. Florescu, A. Săndulescu, D.S. Delion, J.H. Hamilton, A. Ramayya, and W. Greiner, Phys. Rev. **C61**, 051602(R) (2000).
- [14] D.S. Delion, A. Florescu and A. Săndulescu, Phys. Rev. **C63**,044312 (2001).
- [15] F. Cârstoiu and R.J. Lombard, Ann. Phys. (N.Y.) **217**, 279 (1992).
- [16] G. Bertsch, J. Borysowicz, H. McManus, and W.G. Love, Nucl. Phys. A **284**, 399 (1977).
- [17] Ş. Mişicu, A. Săndulescu, G.M. Ter-Akopian, and W. Greiner, Phys. Rev. C **60**, 034613-6 (1999).
- [18] D.A.Varshalovitch, A.N.Moskalev and V.K.Hersonsky, Quantum Theory of Angular Momentum (in russian), (Nauka , Leningrad, 1975).

- [19] D.S. Delion, A. Săndulescu, Ş Mişicu F. Carstoiu, and W. Greiner, J. Phys G**28**, 289 (2002).
- [20] D.S. Delion, A. Săndulescu, and W. Greiner, J. Phys. G (in press).
- [21] Dao T. Khoa, Phys. Rev. C**63**, 034007 (2000).
- [22] P. Möller, J.R. Nix, W.D. Myers, and W.J. Swyatecki, At. Data Nucl. Data Tables **59**, 185 (1995).
- [23] A. Săndulescu, Ş. Mişicu, F. Cârstoiu, A. Florescu, and W. Greiner, Phys. Rev. C **58**, 2321 (1998).
- [24] D.S. Delion, A. Insolia, and R.J. Liotta, Phys. Rev. C**46**, 884 (1992).

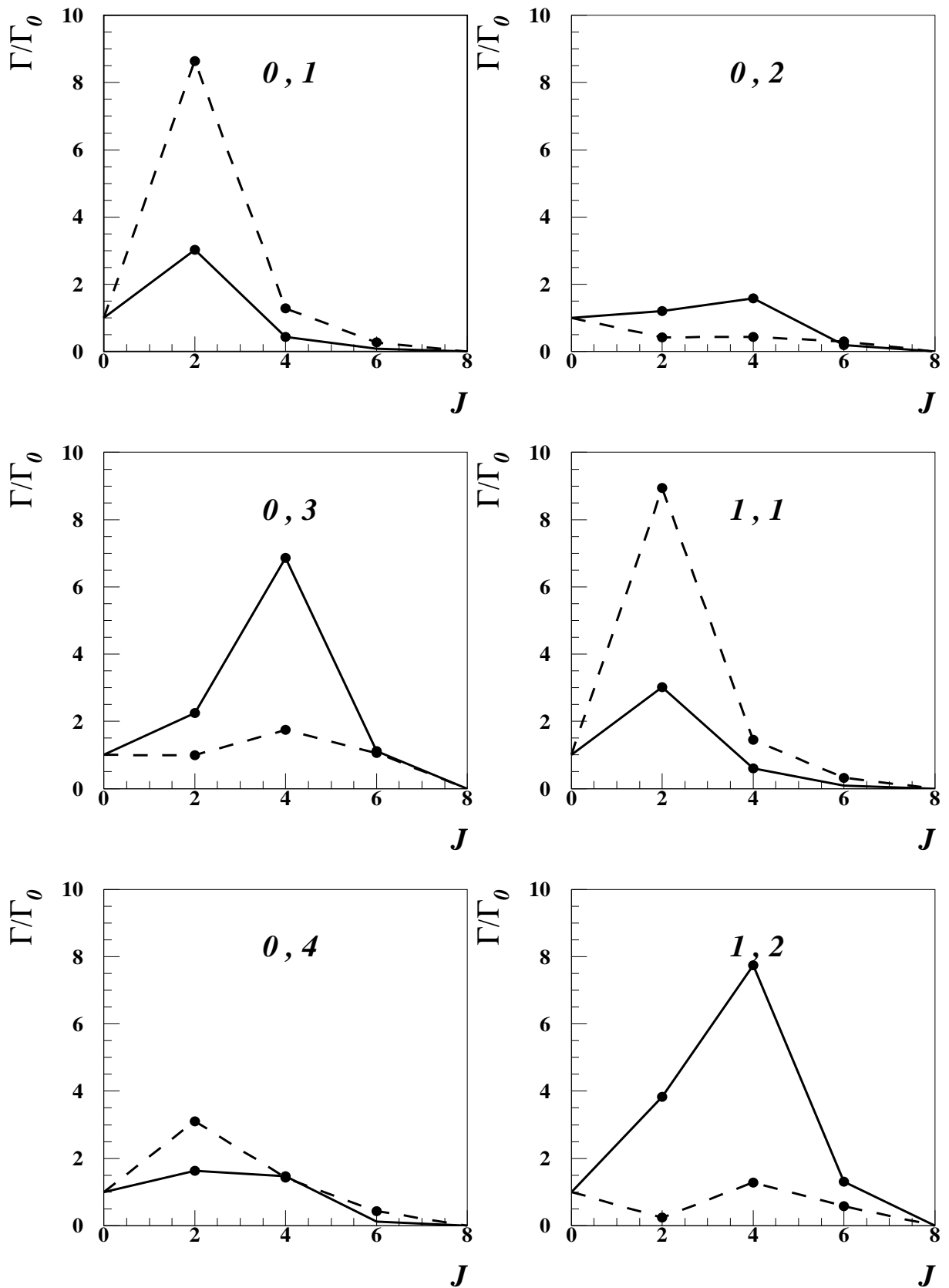


Figure 1: Total widths per nucleus versus the final spin for  $^{104}\text{Mo}$  (solid lines) and  $^{148}\text{Ba}$  (dashed lines).

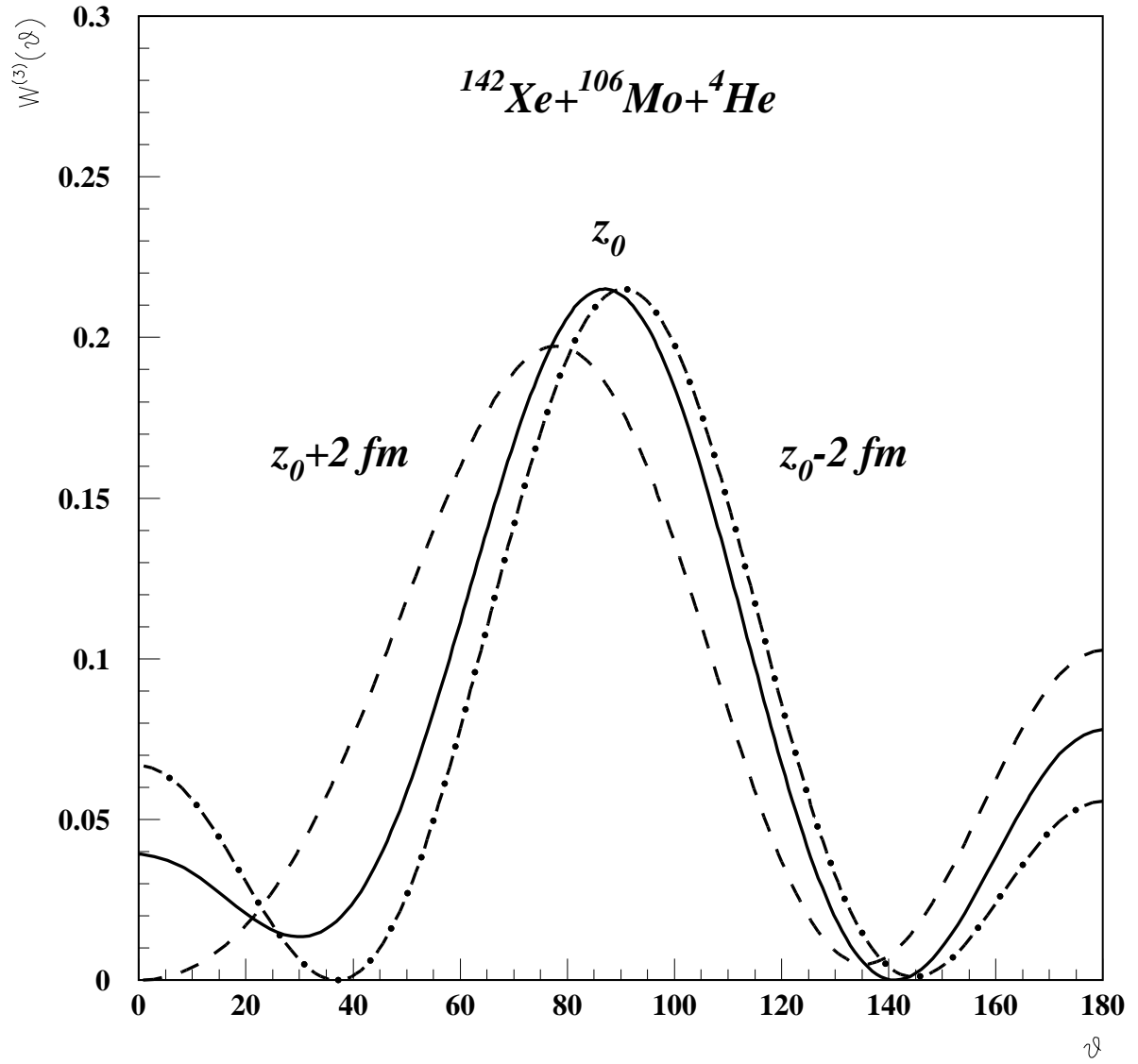


Figure 2: Normalized angular distribution of the process (A) for  $z_0$  (solid line),  $z_0 + 2 \text{ fm}$  (dashed line) and  $z_0 - 2 \text{ fm}$  (dot-dashed line). The parameters of the nuclear potential are  $V_0=27.7 \text{ MeV}$ ,  $R=15 \text{ fm}$ ,  $x_0=6 \text{ fm}$ .